Vector solitons in nonlocal optical media with pseudo spin-orbit-coupling

Huagang Li (李华刚),[1] Xi Peng (彭喜),[1] and Zhiwei Shi (石智伟)[2,*]

[1]*School of Photoelectric Engineering, Guangdong Polytechnic Normal University, Guangzhou 510665, China*

[2]*School of Electro-mechanical Engineering, Guangdong University of Technology, Guangzhou 510006, China*

(Received 13 August 2020; revised 27 December 2020; accepted 15 January 2021; published 5 February 2021)

We numerically investigate the existence and stability of nonlocal vector solitons with pseudo spin-orbit-coupling (SOC). The pseudo SOC is realized by a framework based on the spatial-domain copropagation of two beams with mutually orthogonal polarizations and opposite transverse components of the carrier wave vectors in nonlocal optical media. The numerical results show that there are two kinds of solutions for vector solitons, one is central symmetric, and the other is noncentral symmetric. The solitons may exist below a certain threshold value of the effective SOC strength in the system.

DOI: 10.1103/PhysRevE.103.022205

I. INTRODUCTION

Ultracold boson gases provide a common platform for simulating many fundamental phenomena in quantum optics and condensed matter physics [1,2]. SOC is one of the important causes of many physical phenomena, but in real physics, the strength of SOC mainly depends on the material parameters, and its tunability is very small or not at all. In 2011, the NIST research team experimentally achieved SOC in Bose-Einstein condensate (BEC) [3], this discovery provides a new experimental platform for regulating SOC and its related physical phenomena [4–9]. Moreover, it is extremely important to carry out related research in other systems to expand the research universality in the field of SOC.

The field of photonics offers a wide variety of options to simulate basic effects known in other areas of physics. In recent years, the study of pseudo SOC in the field of optics has also been reported. The spatiotemporal light bullets were studied in dual-core optical waveguides with the intrinsic self-focusing [10], which is based on the remarkable mechanism of the stabilization of two-dimensional (2D) solitons in BEC with the attractive intrinsic nonlinearity [11]. SOC is well known because it resembles intermodal dispersion (also known as dispersion coupling) in optics [12–15]. However, the Gross-Pitaevskii equation in BEC with SOC is very different from the transmission equation in Ref. [10]. The nonlinear part of Gross-Pitaevskii equation in BEC is similar to the Manakov system in nonlinear optics [16,17], and the corresponding physical model can be optical fiber arrays [16] or birefringence fibers [17]. However, the experimental method to realize the adjustable intermodal dispersion in optical fiber is more complicated.

Based on the similarity of laser transmission in space and optical fiber, studies have also been reported to simulate SOC in BEC by laser transmission in space [18]. In the framework based on the spatial-domain copropagation of two light beams with mutually orthogonal polarizations and opposite transverse components of carrier wave vectors in the local nonlinear media with randomly varying birefringence, the solitons were gained with pseudo SOC [18]. And this research results from the similarity between fundamental dynamical equations governing the excitation of matter waves in BEC (the Gross-Pitaevskii equation) and the propagation of waves in optics (the nonlinear Schrödinger equation). Some relevant theoretical research results in BEC can be experimentally verified in optics. In the experimental frame, only basic diffraction is considered for laser transmission in space, which is different from that in optical fiber. In other words, vanishing coupling or higher-order dispersion coupling in the vector system can be reasonably ignored. Next, linear polarized light can be decomposed into linear superposition of left-polarized light and right-polarized light, which is the basis for realizing pseudo SOC in this kind of Manakov system [18,19]. Though SOC cannot be realized in vector systems in optics as of now though the term has been already introduced in systems such as fiber couplers, the original motivation is of emulation of SOC in Manakov-like systems theoretically here. When circularly polarized component beams describe cross propagation of orthogonal polarized vector beams, linear terms similar to spin orbit coupling effects in mathematical form are derived from the equations. Of course, how to implement it in experiments remains to be studied.

Compared with the local nonlinear optical medium, the nonlocal nonlinear optical medium has many remarkable characteristics. For example, the nonlocal nonlinear Schrödinger equation (NNLS) is approximated as a linear model under the strong nonlocal condition [20], and the nonlocal nonlinear medium can avoid the two-dimensional beam collapse [21]. Nonlocal nonlinear media have been playing an important role in the field of nonlinear optics after more than 20 years' development. People have also found some interesting phenomena, such as 2D accessible solutions in parity-time symmetric potentials [22], modular installation [23], and modulation instability in nonlocal Kerr media [24], nonlocal surface wave solutions [25], and stabilization of vector soliton complexes [26], etc. More fortunately, in most isotropic nonlocal media, the nonlinear effect is similar to

*szwstar@gdut.edu.cn

that of Manakov system for the transmission of orthogonal polarization vector beams [26], so the random birefringence medium required by local nonlinear medium is avoided, and it is a real natural physical system that can be easily obtained. The huge class of parametric nonlinearities, such as quadratic nonlinear materials, whose nonlinearity is also nonlocal [27], which has, e.g., enabled the prediction of good regimes for quadratic soliton pulse compression [28,29]. The nonlocal nature of the quadratic nonlinearity in fact also explains the existence of the beautiful X wave [30]. Very appropriately the response function of parametric interaction is also exponential [31–34] as the model we use here. For a more detailed discussion of wide applications of nonlocality, see Ref. [35] for a review.

Intermodal dispersion exists in fiber couplers [12–15], but it has little influence on the switching characteristics of fiber couplers [13], and the realization of optical switching phenomenon mainly depends on the linear coupling coefficient [19]. The cross-transmission physical framework of orthogonal polarization vector beam in Ref. [18] can obviously realize the optical switching phenomenon, but the realization of the optical switching phenomenon mainly depends on the pseudo SOC, rather than the linear coupling coefficient or the Rabi coupling. Therefore, the optical switching phenomenon can also be realized when the nonlocal medium adopts cross transmission of orthogonal polarization vector beam, and there is no linear coupling coefficient or the Rabi coupling because the isotropic medium is adopted.

II. THEORY MODEL AND NUMERICAL RESULTS

This work aims to simulate SOC effects by designing an optical development framework in a nonlocal optical medium. We consider copropagation of optical beams with orthogonal linear polarizations in the isotropic nonlocal medium. Thus, the electric constituent of the electromagnetic field can be taken as

$$\mathbf{E}(x,z,t)=\tfrac{1}{2}[\mathbf{e}_xE_x(x,z,t)+\mathbf{e}_yE_y(x,z,t)]+\text{c.c.} \tag{1}$$

where $\mathbf{e}_{x,y}$ denotes unit vectors transverse to the propagation axis z, E_x, and E_y being complex amplitudes of the respective field components, while x is the transverse coordinate, and c.c. indicates the complex-conjugate contribution. Further, we can write the field components in Eq. (1) as

$$E_x=A_xe^{ik_zz+ik_xx-i\omega t},\quad E_y=A_ye^{ik_zz-ik_xx-i\omega t}, \tag{2}$$

assuming opposite signs of the x components of their wave vectors, which are related to the carrier wavelength, $\sqrt{k_x^2+k_z^2}=2\pi n_0/\lambda$, ω and n_0 being the respective frequency and the background refractive index, respectively. In the usual paraxial approximation [36], the coupled NNLS equations for slowly varying amplitudes from Eqs. (1) and (2) are gotten [26],

$$\begin{aligned}
&2ik_z\frac{dA_x}{dz}+2ik_x\frac{\partial A_x}{\partial x}+\frac{\partial^2A_x}{\partial x^2}+2k_0^2n_0n_2A_x\int_{-\infty}^{\infty}R(x-\tau)[|A_x(\tau)|^2+|A_y(\tau)|^2]d\tau=0,\\
&2ik_z\frac{dA_y}{dz}-2ik_x\frac{\partial A_y}{\partial x}+\frac{\partial^2A_y}{\partial x^2}+2k_0^2n_0n_2A_y\int_{-\infty}^{\infty}R(x-\tau)[|A_x(\tau)|^2+|A_y(\tau)|^2]d\tau=0.
\end{aligned} \tag{3}$$

Here, the nonlocality of the materials is supposed to be ruled with an exponential response function $R(x)=1/(2d^{1/2})\exp(-|x|/d^{1/2})$, where d is the degree of the nonlocality.

Assuming $Q^+=(A_x+iA_y)/\sqrt{2}$, $Q^-=(A_x-iA_y)/\sqrt{2}$, Eq. (3) is transformed into a system with linear couplings, denoted by the field variables and their first x derivatives:

$$\begin{aligned}
&2ik_z\frac{dQ^+}{dz}+2ik_x\frac{\partial Q^-}{\partial x}+\frac{\partial^2Q^+}{\partial x^2}+2k_0^2n_0n_2Q^+\int_{-\infty}^{\infty}R(x-\tau)[|Q^+(\tau)|^2+|Q^-(\tau)|^2]d\tau=0,\\
&2ik_z\frac{dQ^-}{dz}+2ik_x\frac{\partial Q^+}{\partial x}+\frac{\partial^2Q^-}{\partial x^2}+2k_0^2n_0n_2Q^+\int_{-\infty}^{\infty}R(x-\tau)[|Q^+(\tau)|^2+|Q^-(\tau)|^2]d\tau=0.
\end{aligned} \tag{4}$$

Then, when we introduce some normalized variables, $q^+=w_0k_0\sqrt{n_0n_2}Q^+$, $q^-=w_0k_0\sqrt{n_0n_2}Q^-$, $\xi=x/w_0$, $\zeta=z/(k_zw_0^2)$, where w_0 is a scale factor, we can get the final form of the NNLS system,

$$\begin{aligned}
&i\frac{dq^+}{d\zeta}+i\alpha\frac{\partial q^-}{\partial\xi}+\frac{1}{2}\frac{\partial^2q^+}{\partial\xi^2}+q^+\int_{-\infty}^{\infty}R(\xi-s)[|q^+(s)|^2+|q^-(s)|^2]ds=0,\\
&i\frac{dq^-}{d\zeta}+i\alpha\frac{\partial q^+}{\partial\xi}+\frac{1}{2}\frac{\partial^2q^-}{\partial\xi^2}+q^-\int_{-\infty}^{\infty}R(\xi-s)[|q^+(s)|^2+|q^-(s)|^2]ds=0,
\end{aligned} \tag{5}$$

where $\alpha=k_xw_0$ is a free parameter, which measures the effective SOC strength in the system [18,37].

We search for stationary soliton solutions of Eq. (5) in the form of $q^\pm(\xi,\zeta)=u^\pm(\xi)e^{ib\zeta}$, where b is a real propagation constant, and complex functions $u^\pm$ satisfy equations

$$\begin{aligned}
&-bu^++i\alpha\frac{\partial u^-}{\partial\xi}+\frac{1}{2}\frac{\partial^2u^+}{\partial\xi^2}+u^+\int_{-\infty}^{\infty}R(\xi-s)[|u^+(s)|^2+|u^-(s)|^2]ds=0,\\
&-bu^-+i\alpha\frac{\partial u^+}{\partial\xi}+\frac{1}{2}\frac{\partial^2u^-}{\partial\xi^2}+u^-\int_{-\infty}^{\infty}R(\xi-s)[|u^+(s)|^2+|u^-(s)|^2]ds=0.
\end{aligned} \tag{6}$$

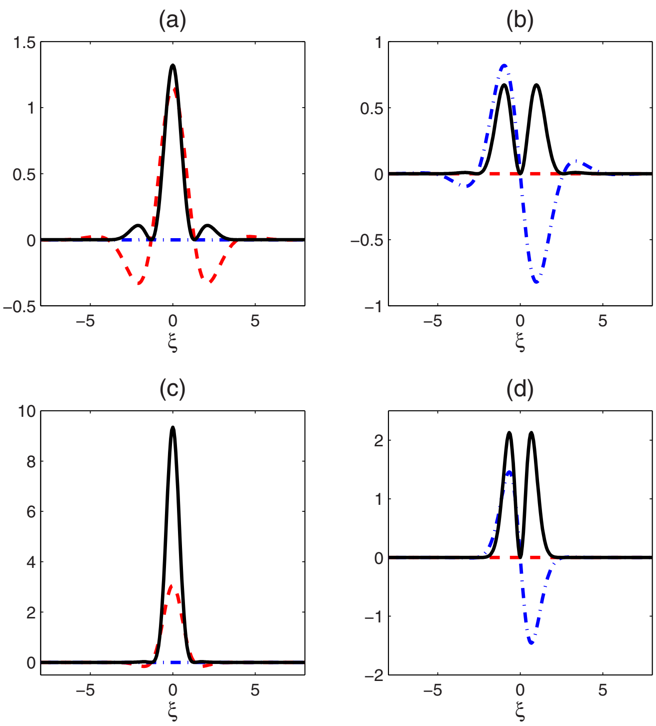

FIG. 1. Complex functions (a) u^+ and (b) u^-, obtained as a numerical solution of Eq. (6) with $\alpha = 1.2$, $d = 1$, and $b = 1.3$. (c) and (d): the same for $b = 4$. Red dashed, blue dashed-dotted, and black solid lines display, respectively, the real part, imaginary part, and squared absolute value of solutions. All quantities are plotted in arbitrary dimensionless units.

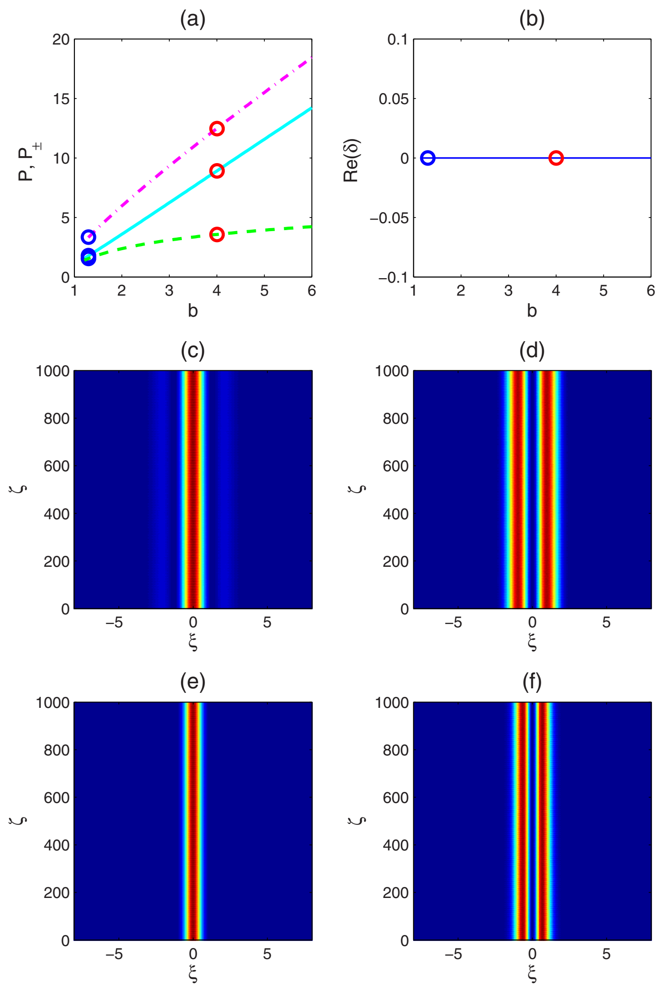

FIG. 2. (a) The powers of each component, P^+, P^-, and the total power, P (cyan solid, green dashed, and magenta dashed-dotted lines, respectively) and (b) the stability parameter $\mathrm{Re}(\delta)$ versus propagation constant b for $\alpha = 1.2$ and $d = 1$ in Eq. (6). The blue and red circles correspond to the solitons shown in Figs. 1(a), 1(b) and 1(c), 1(d), respectively. (c)–(f) Results of direct simulations, displayed by means of the spatiotemporal distribution of the density of the evolution of the soliton with random-noise perturbations added at the 5% amplitude level. (c) and (d) correspond to Figs. 1(a) and 1(b), respectively; (e) and (f) correspond to Figs. 1(c) and 1(d), respectively. All quantities are plotted in arbitrary dimensionless units.

To find soliton solutions of Eq. (6), we used the known squared-operator method [38]. There will be a balance between the pure real solution and the pure imaginary solution for u^+ and u^- in Eq. (6), respectively. That is, u^+ and $i\partial u^-/\partial x$ are the pure real solution, u^- and $i\partial u^+/\partial x$ are the pure imaginary solution, and vice versa. And the typical solutions are shown in Figs. 1(a)–1(d). We can see that u^+ is the pure real solution and u^- is the pure imaginary solution. When the propagation constant b is smaller, there will be some small peaks at the edge of the beam, to see Figs. 1(a) and 1(b).

The curve of the soliton's total power $P = P_+ + P_-$ ($P_\pm = \int_{-\infty}^{\infty} |u^\pm|^2 d\xi$) versus the propagation constant b, represents a monotonously increasing function, see Fig. 2(a). The difference between power P_+ and P_- increases with the increase of propagation constant b.

We further carry out stability analysis for the solitons against small perturbations by means of the linearization procedure. For a given stationary soliton, $q^\pm(\xi,\zeta) = u^\pm(\xi)e^{ib\zeta}$, small perturbations are added as $q^\pm(\xi,\zeta) = [u^\pm + \epsilon F^\pm e^{\delta\zeta} + \epsilon(G^\pm)^* e^{\delta^*\zeta}]e^{ib\zeta}$ with infinitesimal amplitude ϵ, where $F^\pm$ and $G^\pm$ are perturbation eigenfunctions, δ is the corresponding growth rate, and "$*$" stands for the complex conjugation. If there is at least one solution with $\mathrm{Re}(\delta) > 0$, the soliton is unstable. The following linearized equations are thus gotten from Eq. (5):

$$-i\delta F^+ = LF^+ + i\alpha\frac{\partial F^-}{\partial x} + \rho F^- + gu^+\Delta n,$$

$$-i\delta G^+ = -LG^+ + i\alpha\frac{\partial G^-}{\partial x} - \rho G^- - g(u^+)^*\Delta n,$$

$$-i\delta F^- = LF^- + i\alpha\frac{\partial F^+}{\partial x} + \rho F^+ + gu^-\Delta n,$$

$$-i\delta G^- = -LG^- + i\alpha\frac{\partial G^+}{\partial x} - \rho G^+ - g(u^-)^*\Delta n, \quad (7)$$

where $L = (1/2)\partial^2/\partial\xi^2 - b + g\int_{-\infty}^{\infty} R(\xi - s)(|u^+(s)|^2 + |u^-(s)|^2)ds$, $\Delta n = \int_{-\infty}^{\infty} R(\xi - s)\{[u^+(s)]^* F^+(s) + u^+(s) G^+(s) + [u^-(s)]^* F^-(s) + u^-(s)G^-(s)\}ds$. The Fourier collocation method can be used to solve Eq. (7) numerically [39]. Numerical results demonstrates that the solitons can be stable, see Fig. 2(b). In the numerical simulation, the window range is 10π, the number of points is 512, and the transmission step is 5×10^{-4}. In order to check the robustness of this soliton species, we carry out simulating its

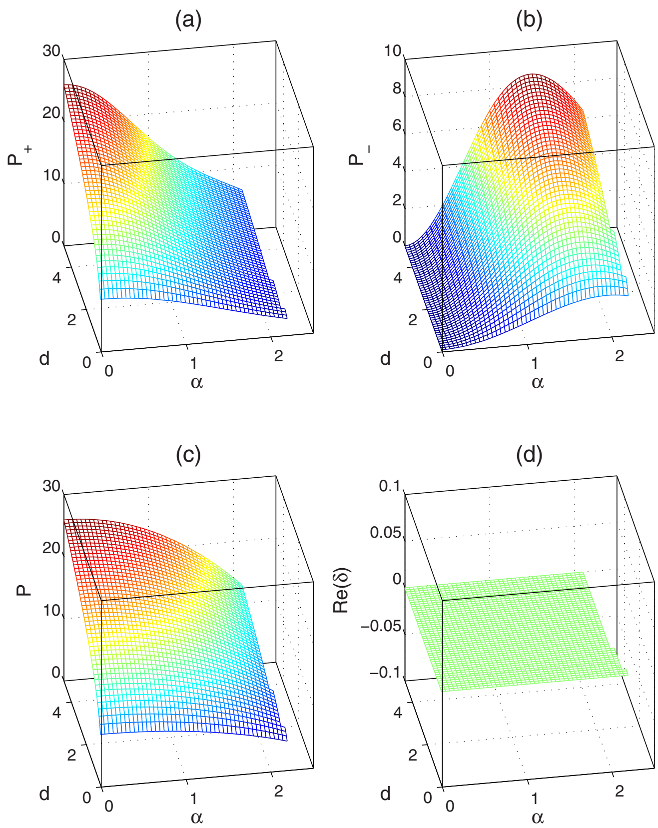

FIG. 3. (a)–(c) The powers of each component, P^+, P^-, and the total power, P, versus the SOC strength α and the degree of the nonlocality d, respectively. (d) The stability parameter Re(δ) versus versus the SOC strength α and the degree of the nonlocality d. Other parameter: $b = 4$. All quantities are plotted in arbitrary dimensionless units.

evolution with the addition of 5% random-noise perturbations The additional random perturbation of the initial beam is $q^{+'} = q^+[1 + 0.05\delta(\xi)]$ and $q^{-'} = q^-[1 + 0.05\delta(\xi)]$, where $\delta(\xi)$ is the random function, which is a homogeneous distributed random recurrence of a real and imaginary part. The beam can be fully described by amplitude and phase, and the formula for additional noise shows that the amplitude and phase of the beam are added to the noise, which can represent all the noise sources, and of course, the quantum noise and amplitude noise are included [40]. The results, shown in Figs. 2(c)–2(f), corroborate the stability predicted by the linear-stability analysis.

We calculate the dependence of the soliton power on the SOC strength α and the degree of the nonlocality d as shown in Figs. 3(a)–3(c), which shows that the soliton exists below a certain threshold value $\alpha \approx 2.2$. And the threshold value increases slowly with the decrease of the degree of the nonlocality d. Above the threshold, the nonlocal nonlinear self-focusing effect can not balance the walk away effect, which are driven by SOC and diffraction effect. We have performed the linear-stability analysis for the solitons, and the results presented in Fig. 3(d) demonstrate that the solitons are stable in the region where they exist.

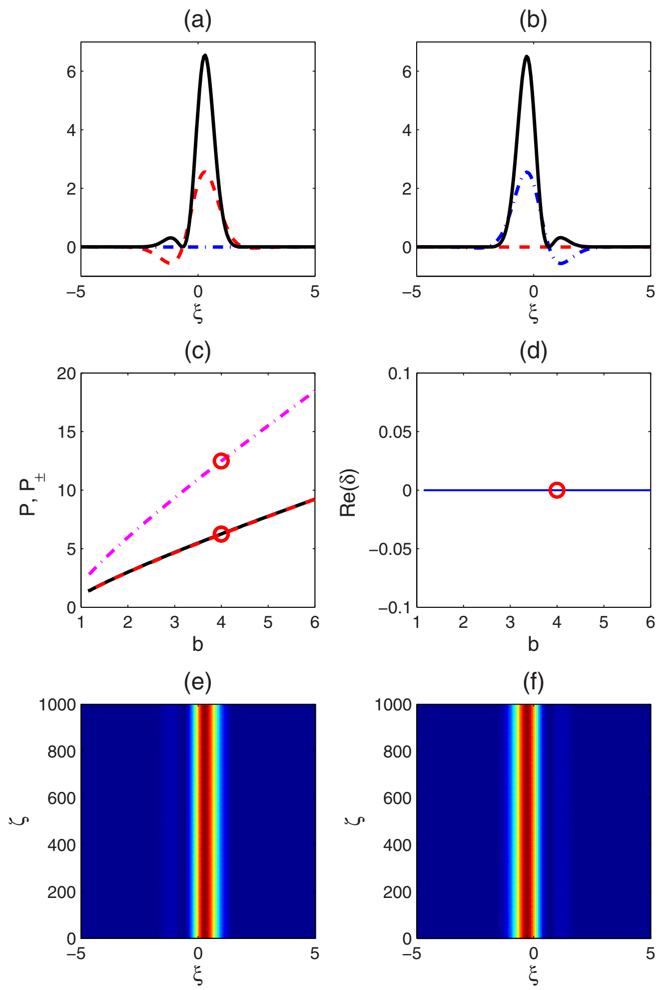

FIG. 4. Complex functions (a) u^+ and (b) u^- obeying the cross-symmetry relation, obtained as a numerical solution of Eq. (6) with $\alpha = 1.2$, $d = 1$, and $b = 4$. Red dashed, blue dashed-dotted, and black solid lines display, respectively, the real part, imaginary part, and squared absolute value of solutions. (c) The powers of each component, P^+, P^-, and the total power, P (black solid, red dashed, and magenta dashed-dotted lines, respectively) and (d) the stability parameter Re(δ) versus propagation constant b for $\alpha = 1.2$ and $d = 1$. The red circles correspond to the soliton shown in (a) and (b). (e) and (f) Results of direct simulations, displayed by means of the spatiotemporal distribution of the density of the evolution of the soliton with random-noise perturbations added at the 5% amplitude level. (e) and (f) correspond to (a) and (b), respectively. All quantities are plotted in arbitrary dimensionless units.

Next, we address solitons with pure real and imaginary components obeying the cross-symmetry relation [18,37]. The typical solitons are shown in Figs. 4(a) and 4(b), and u^+ is the pure real solution and u^- is the pure imaginary solution. The curve of the power $P_\pm$ versus propagation constant b is shown that $P_+ \approx P_-$, to see Fig. 4(c). We have performed the linear-stability analysis for the solitons, and the results presented in Fig. 4(d) demonstrate that the solitons are stable in the region where they exist. We have also checked the robustness of this soliton species by simulating its evolution with the addition of 5% random-noise perturbations. The results, illustrated by

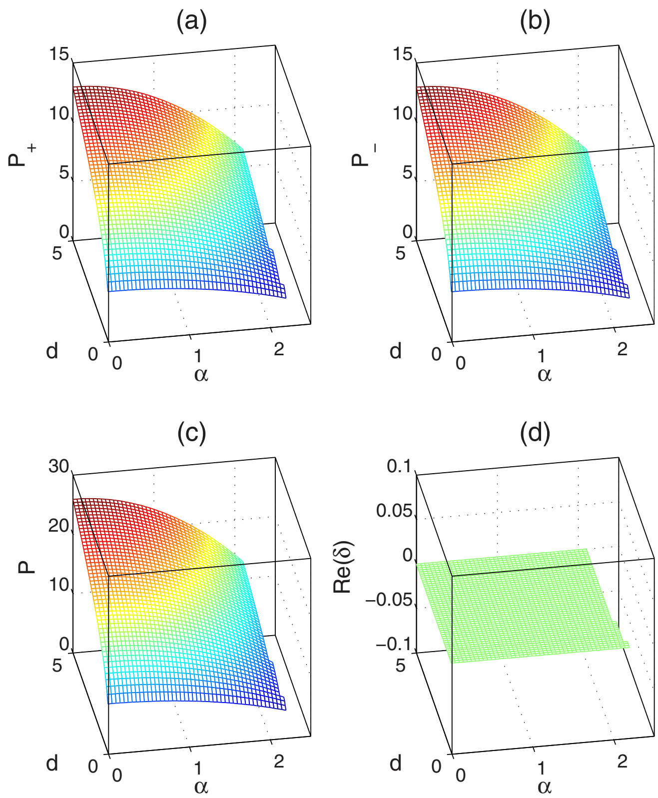

FIG. 5. (a)–(c) The powers of pure real and imaginary components obeying the cross-symmetry relation, P^+, P^-, and the total power, P, versus the SOC strength α and the degree of the nonlocality d, respectively. (d) The stability parameter Re(δ) versus versus the SOC strength α and the degree of the nonlocality d. Other parameter: $b = 4$. All quantities are plotted in arbitrary dimensionless units.

Figs. 4(e) and 4(f), corroborate the stability predicted by the linear-stability analysis.

Figures 5(a)–5(c) shows the dependence of the power of the soliton with pure real and imaginary components obeying the cross-symmetry relation on the SOC strength α and the degree of the nonlocality d. Comparing Figs. 5(b) and 5(c) with Figs. 3(b) and 3(c), they are clearly different. In Figs. 3(b) and 3(c), P_+ and P_- change differently when α and d change. However, we can see that P_+ and P_- remain approximately equal when α and d change in Figs. 5(b) and 5(c). Moreover, the soliton may also exist below a certain threshold value ($\alpha \approx 2.2$), which increases slowly with the decrease of the degree of the nonlocality d. By doing the linear-stability analysis for the solitons, we have found that the solitons are also stable if they exist, as presented in Fig. 5(d).

III. CONCLUSION

In conclusion, we have obtained the vector solitons in nonlocal optical media with pseudo spin-orbit-coupling. The effective SOC interaction between two copropagating beams is induced by opposite transverse components of their wave vectors. Numerical results demonstrate the existence of families of stable solitons in this optical system. As an extension of the work, it will be interesting to develop it for the spatial-domain propagation in the bulk medium, which may help to emulate two-dimensional nonlocal matter-wave solitons in the optical settings.

ACKNOWLEDGMENTS

This work was supported by the Guangdong Basic and Applied Basic Research Foundation (Grants No. 2016A030313747 and No. 2020A1515010623), National Natural Science Foundation of China (Grant No. 11764022) and the Theoretical Physics Program of National Natural Science Foundation of China (Grants No. 11947103).

[1] P. Hauke, F. M. Cucchietti, L. Tagliacozzo, I. Deutsch, and M. Lewenstein, Can one trust quantum simulators? Rep. Prog. Phys. **75**, 082401 (2012).
[2] T. H Johnson, S. R. Clark, and D. Jaksch, What is a quantum simulator? EPJ Quant. Technology **1**, 10 (2014).
[3] Y.-J. Lin, K. Jiménez-García, and I. B. Spielman, Spin-orbit-coupled Bose-Einstein condensates, Nature (London) **471**, 83 (2011).
[4] N. Goldman, G. Juzeliūnas, P. Öhberg, and I. B. Spielman, Light-induced gauge fields for ultracold atoms, Rep. Prog. Phys. **77**, 126401 (2014).
[5] E. Zohar, J. I. Cirac, and B. Reznik, Quantum simulations of lattice gauge theories using ultracold atoms in optical lattices, Rep. Prog. Phys. **79**, 014401 (2016).
[6] M. Aidelsburger, Artificial gauge fields and topology with ultracold atoms in optical lattices, J. Phys. B: At. Mol. Opt. Phys. **51**, 193001 (2018).
[7] V. Galitski, G. Juzeliūnas, and I. B. Spielman, Artificial gauge fields with ultracold atoms, Phys. Today **72**, 38 (2019).
[8] N. Goldman, J. C. Budich, and P. Zoller, Topological quantum matter with ultracold gases in optical lattices, Nature Phys. **12**, 639 (2016).
[9] N. R. Cooper, T. C. M. Group, J. Dalibard, and I. B. Spielman, Topological bands for ultracold atoms, Rev. Mod. Phys. **91**, 015005 (2019).
[10] Y. V. Kartashov, B. A. Malomed, V. V. Konotop, V. E. Lobanov, and L. Torner, Stabilization of spatiotemporal solitons in Kerr media by dispersive coupling, Opt. Lett. **40**, 1045 (2015).
[11] H. Sakaguchi, B. Li, E. Ya. Sherman, and B. A. Malomed, Composite solitons in two-dimensional spin-orbit coupled self-attractive Bose-Einstein condensates in free space, Rom. Rep. Phys. **70**, 502 (2018).
[12] K. S. Chiang, Intermodal dispersion in two-core optical fibers, Opt. Lett. **20**, 997 (1985).
[13] A. K. Sarma, Dark soliton switching in an NLDC in the presence of higher-order perturbative effects, Opt. Laser Technol. **41**, 247 (2009).

[14] A. Govindaraji, A. Mahalingam, and A. Uthayakumar, Femtosecond pulse switching in a fiber coupler with third order dispersion and self-steepening effects, Optik **125**, 4135 (2014).
[15] A. Govindaraji, A. Mahalingam, and A. Uthayakumar, Dark soliton switching in nonlinear fiber couplers with gain, Opt. Laser Technol. **60**, 18 (2014).
[16] T. Kanna and M. Lakshmanan, Exact Soliton Solutions, Shape Changing Collisions, and Partially Coherent Solitons in Coupled Nonlinear Schrödinger Equations, Phys. Rev. Lett. **86**, 5043 (2001).
[17] R. Radhakrishnan and M. Lakshmanan, Exact soliton solutions to coupled nonlinear Schrödinger equations with higher-order effects, Phys. Rev. E **54**, 2949 (1996).
[18] H. Li, X. Zhu, B. A. Malomed, D. Mihalache, Y. He, and Z. Shi, Emulation of spin-orbit coupling for solitons in nonlinear optical media, Phys. Rev. A **101**, 053816 (2020).
[19] G. P. Agrawal, *Nonlinear Fiber Optics*, 4th Ed. (Academic Press, San Diego, 2007).
[20] A. W. Snyder and D. J. Mitchell, Accessible solitons, Science **276**, 1538 (1997).
[21] O. Bang, W. Krolikowski, J. Wyller, and J. J. Rasmussen, Collapse arrest and soliton stabilization in nonlocal nonlinear media, Phys. Rev. E **66**, 046619 (2002).
[22] B. Yang, W. P. Zhong, and M. R. Belic, Self-similar Hermite-Gaussian spatial solitons in two-dimensional nonlocal nonlinear media, Commun. Theor. Phys. **53**, 937 (2010).
[23] W. P. Zhong, M. R. Belic, and T. W. Huang, Two-dimensional accessible solitons in PT-symmetric potentials, Nonlinear Dyn. **70**, 2027 (2012).
[24] J. Wyller, O. Bang, W. Krolikowski, and J. J. Rasmussen, Generic features of modulational instability in nonlocal Kerr media, Phys. Rev. E **66**, 066615 (2002).
[25] B. Alfassi, C. Rotschild, O. Manela, M. Segev, and D. N. Christodoulides, Nonlocal Surface-Wave Solitons, Phys. Rev. Lett. **98**, 213901 (2007).
[26] Z. Xu, Y. V. Kartashov, and L. Torner, Stabilization of vector soliton complexes in nonlocal nonlinear media, Phys. Rev. E **73**, 055601(R) (2006).
[27] N. I. Nikolov, D. Neshev, O. Bang, and W. Z. Królikowski, Quadratic solitons as nonlocal solitons, Phys. Rev. E **68**, 036614 (2003).
[28] M. Bache, O. Bang, J. Moses, and F. W. Wise, Nonlocal explanation of stationary and nonstationary regimes in cascaded soliton pulse compression, Opt. Lett. **32**, 2490 (2007).
[29] M. Bache, O. Bang, W. Krolikowski, J. Moses, and F. W. Wise, Limits to compression with cascaded quadratic soliton compressors, Opt. Express **16**, 3273 (2008).
[30] P. V. Larsen, M. P. Sørensen, O. Bang, W. Z. Królikowski, and S. Trillo, Nonlocal description of X waves in quadratic nonlinear materials, Phys. Rev. E **73**, 036614 (2006).
[31] P. D. Rasmussen, O. Bang, and W. Królikowski, Theory of nonlocal soliton interaction in nematic liquid crystals, Phys. Rev. E **72**, 066611 (2005).
[32] W. Królikowski, O. Bang, and J. Wyller, Nonlocal incoherent solitons, Phys. Rev. E **70**, 036617 (2004).
[33] Q. Kong, Q. Wang, O. Bang, and W. Krolikowski, Analytical theory for the dark-soliton interaction in nonlocal nonlinear materials with an arbitrary degree of nonlocality, Phys. Rev. A **82**, 013826 (2010).
[34] Q. Kong, Q. Wang, O. Bang, and W. Krolikowski, Analytical theory of dark nonlocal solitons, Opt. Lett. **35**, 2152 (2010).
[35] W. Królikowski, O. Bang, N. I. Nikolov, D. Neshev, J. Wyller, J. J. Rasmussen, and D. Edmundson, Modulational instability, solitons and beam propagation in nonlocal nonlinear media, J. Opt. B: Quantum Semiclass. Opt. **6**, S288 (2004).
[36] Y. S. Kivshar and G. P. Agrawal, *Optical Solitons: From Fibers to Photonic Crystals* (Academic Press, San Diego, 2003).
[37] Y. V. Kartashov, V. V. Konotop, and F. Kh. Abdullaev, Gap Solitons in a Spin-Orbit-Coupled Bose-Einstein Condensate, Phys. Rev. Lett. **111**, 060402 (2013).
[38] J. Yang and T. I. Lakoba, Universally-convergent squared-operator iteration methods for solitary waves in general nonlinear wave equations, Stud. Appl. Math. **118**, 153 (2007).
[39] J. Yang, *Nonlinear Waves in Integrable and Nonintegrable Systems* (SIAM, Philadelphia, 2010).
[40] E. Gernier, P. Bowen, T. Sylvestre, J. M. Dudley, and O. Bang, Amplitude noise and coherence degradation of femtosecond supercontinuum generation in all-normal-dispersion fibers, J. Opt. Soc. Am. B **36**, A161 (2019).